A Numerical Vortex Approach to Aerodynamic Modeling of SUAV/VTOL Aircraft

Douglas Hunsaker
Brigham Young University

Abstract

A numerical lifting line method, coupled with a numerical blade element method, is presented as a low computational cost approach to modeling slipstream effects on a finite wing. This method uses a 3D vortex lifting law along with known 2D airfoil data to predict the lift distribution across a wing in the presence of a propeller slipstream. The results are of significant importance in the development of an aerodynamic modeling package for initial stages of vertical take-off and landing (VTOL) aircraft design. An overview of the algorithm is presented, and results compared with published experimental data.

Nomenclature

A_i	area of wing section i
B_d	slipstream development factor
b	number of propeller blades
c_b	blade section chord
C_{Li}	wing section lift coefficient
C_l	blade section lift coefficient
$\mathbf{d\ell_i}$	wing section differential vortex vector
D_p	propeller diameter
$\mathbf{dF_i}$	wing section differential force vector
dF_i	wing section differential force magnitude
R_p	propeller radius
r	radial distance from propeller axis
s	normal distance to propeller plane
V	blade section total induced velocity
$\mathbf{V_i}$	wing section incident velocity vector
V_i	wing section incident velocity magnitude
V_θ	blade section induced tangential velocity
α_i	wing section angle of attack
β_t	geometric angle of attack at propeller tip
δ_i	wing section flap deflection
ϵ	blade section induced angle of attack
ϵ_∞	blade section advance angle of attack
κ	Goldstein's kappa factor
Γ	blade section circulation
Γ_i	wing section vortex strength
ω	propeller angular velocity
ρ	fluid density
θ	azimuthal angle of propeller

1 Introduction

Aerodynamic modeling of SUAV VTOL aircraft presents unique problems because VTOL aircraft experience aerodynamic forces foreign to conventional aircraft. For example, during take-off, hovering, and landing, propwash effects become dominant while freestream flow from the aircraft's forward velocity is almost negligible. Additionally, current aircraft design tools are almost exclusively based on inviscid flow assumptions, which are questionable for Reynolds numbers less than 800,000, and certainly inadequate for Reynolds numbers less than 200,000. Accounting for viscous effects, at least to some extent, is important in the development of VTOL aircraft, as the wings are often stalled during common maneuvers.

Commonly, computational fluid dynamics (CFD) and/or experimental trial and error are used as design

"tools" for the development of fixed-wing SUAVs. Although relatively accurate, these methods require too much time to be used during initial design phases. Rather, such methods act as viable analysis tools to be employed after a design has reached some level of maturity. A design tool that rapidly and accurately predicts geometry, propwash, and Reynolds number effects on aerodynamic forces and moments is desired.

Blade element theories [1] and helical vortex models[2] have been employed to model propeller induced flowfields with impressive success. These propeller models have been linked with panel methods to predict the aerodynamic influence of a propeller on a wing[3, 4]. An alternative to panel methods has been suggested by Phillips[5] which extends Prandtl's Lifting Line Theory to wings with sweep and washout. Phillips showed that the algorithm matched the accuracy of CFD solutions while requiring only a fraction of the computational cost. However, this extension of the lifting line theory has never been used to predict the effects of propwash on a wing. The method presented here extends the original Lifting Line algorithm to allow viscous effects on the 2D section lift and drag behavior, and the effects of non-uniform airflow over a wing (i.e. propwash effects). This approach, rooted in inviscid theory, accounts for the effects of viscosity on the lift, drag, and moment behavior via semi-empirical corrections to an otherwise potential flow solution.

2 Aero Model Overview

In the numerical lifting line method presented by Phillips[5], a finite wing is modeled using a series of horseshoe vortices with one edge bound to the quarter chord of the wing and the trailing portion aligned with the freestream velocity. A general 3D vortex lifting law is combined with Prandtl's hypothesis that each spanwise section of the wing has a section lift equivalent to that acting on a similar 2D airfoil with the same local angle of attack.

From the 3D vortex lifting law, the differential force vector produced by the finite wing section i is

$$\mathbf{dF_i} = \rho\Gamma_i \mathbf{V_i} \times \mathbf{d\ell_i} \tag{1}$$

The lift coefficient of a 2D airfoil can be expressed as an arbitrary function of angle of attack and flap deflection

$$C_{L_i} = C_{L_i}(\alpha_i, \delta_i) \tag{2}$$

Assuming that this relationship is known at each section, the magnitude of the differential force produced by wing section i is

$$dF_i = \frac{1}{2}\rho V_i^2 C_{L_i}(\alpha_i, \delta_i) A_i \tag{3}$$

Setting the magnitude of Eq. (1) equal to the right hand side of Eq. (3) for each of the spanwise sections of the wing produces a system of equations that can be solved for the vortex strengths at each section. Once all the vortex strengths are known, the force vector at each section can be computed and summed together to determine the force and moment vectors acting on the wing. This method has been shown to work well at predicting the inviscid forces and moments for wings with sweep and dihedral and aspect ratios greater than four. Accuracy is similar to panel methods or Euler computational fluid dynamics, but at a fraction of the cost. In addition, systems of lifting surfaces with arbitrary position and orientation can be analyzed.

3 Propeller Model Overview

In order to predict the time-averaged flowfield behind a propeller, an induced velocity must be known behind the propeller. This velocity is a function of radius if the propeller axis is in line with the freestream velocity vector, and a function of radius and azimuthal angle, θ, if the propeller is not aligned with the freestream. Phillips presents an approach which is not constrained to situations where the freestream velocity is aligned with the propeller axis. Thus, off-axis moments and forces from the propeller can be found. Dividing the propeller into N discrete intervals, the induced velocity at each radial blade element can be found by relating the section circulation to the section induced tangential velocity as shown in Eq. (4).

$$k\Gamma = 4\pi\kappa r V_\theta \tag{4}$$

Substituting Prandtl's tip loss factor[6] for Goldstein's kappa factor, the following equation is produced

$$\frac{\frac{bc_b}{16r}C_l}{-\cos^{-1}\left(exp\left[-\frac{b\left(1-\frac{2r}{D_p}\right)}{2\sin\beta_t}\right]\right)\tan\epsilon\sin(\epsilon_\infty+\epsilon)} = 0 \quad (5)$$

which can be numerically solved for ϵ_i. Once ϵ_i is known for a given blade section, the total induced velocity is found from

$$V = \frac{\omega r\sin\epsilon}{\cos\epsilon_\infty} \quad (6)$$

This velocity vector is then divided into its axial and tangential components.

Once the induced axial and tangential velocities are known at the propeller plane, the flowfield behind the propeller can be estimated by applying momentum equations. The slipstream radius at a distance s behind the propeller is found by solving for the slipstream development factor suggested by McCormick.

$$B_d = 1 + \frac{s}{\sqrt{s^2+R_p^2}} \quad (7)$$

Where B_d is the development factor and approaches 2 as the distance from the propeller plane (s) approaches infinity. Using this radius, and applying conservation of mass and angular momentum as suggested by Stone[7], the development of the axial and tangential velocities throughout the slipstream are found.

4 Model Assumptions

This approach to modeling the propeller flowfield implies a few underlying assumptions.

- The propeller affects the wing, but the wing does not affect the propeller. This allows for the combined aerodynamic and propeller models to first solve the propeller behavior and then solve for the aerodynamics of the wing in the resultant flowfield. No iterations need be performed between the flowfields of the wing and propeller, which provides a quicker solution.
- The axis of the propeller slipstream stays coincident with the axis of the propeller. This can be assumed if the forward velocity of the craft is always much greater than the sideslip velocity.
- There is no mixing between the slipstream and the freestream velocities. No adjustments are made along the edges of the slipstream to account for mixing with the freestream. This is obviously a faulty assumption, but accounting for these effects is beyond the scope of this initial-stage aerodynamic model.

The model used in the following results includes one additional assumption: The resultant induced velocities at any distance behind the propeller were assumed constant with varying azimuthal angle. Therefore, although the induced velocity downstream from the propeller is a function of θ when the propeller is at an angle of attack, the average velocity at that radius and distance from the propeller was taken as the induced velocity.

5 Results

5.1 Aerodynamic Model Validation

As a first check on the algorithm, inviscid estimates of wing lift and induced drag coefficient for straight and swept wings in a uniform freestream were computed. The section lift coefficient was defined as a linear function of angle of attack, and the section parasite drag was set to zero. For this case, this algorithm exactly reproduces the results of the original numerical lifting line algorithm[5].

To determine the ability of this method to predict the effects of the propeller slipstream, results have been compared to the experimental data of Stuper[8]. Figure 1 illustrates the model geometry, showing the wing, end caps, and representative size of the slipstream. Note that the chord-wise lines represent the distribution of the 2D spanwise wing sections.

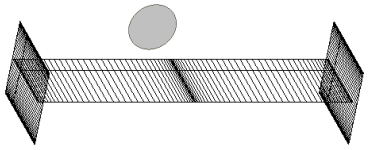

Figure 1: Computer model of finite wing showing distribution of the spanwise sections and the end-cap geometry.

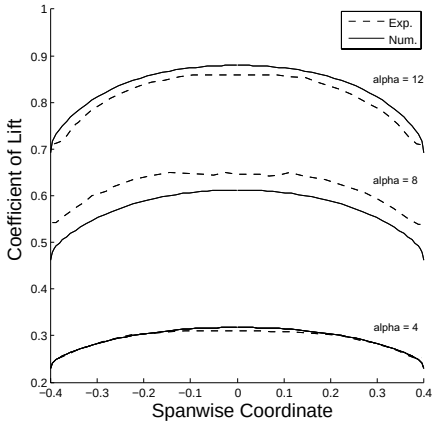

Figure 2: C_L distribution across the wing span at three angles of attack with a uniform freestream velocity.

Figure 2 shows a comparison of the resulting numerical solutions with the experimental C_L distributions at three angles of attack. Note that the C_L distribution across the entire wing at both 4° and 12° angle of attack agree almost completely. At $\alpha = 8°$, however, the C_L distribution is under-predicted. This discrepancy is a result of a "jump" in the experimentally measured lift that occurs near $\alpha = 8°$. This "jump" is not predicted by the 2D airfoil RANS solution used as the C_l vs α input into the lifting line algorithm.

5.2 Propeller Model Validation

Results from the model are first shown vs. experimental results published by Kotb[9]. Kotb included many important parameters in his paper, which allowed for accurate propeller parameters to be used in the numerical model. However, airfoil lift and drag were assumed to match a NACA 0012 airfoil. Figure 3 displays the numerical vs. experimental values for coefficient of thrust vs. advance ratio. The numerical model appears to be slightly optimistic for the predicted thrust coefficient across the entire range of tested advance ratios. This could be due to the fact that the model makes no adjustment for mixing with the freestream at the boundaries of the propwash. The inability to account for the mixing phenomena is apparent in subsequent plots.

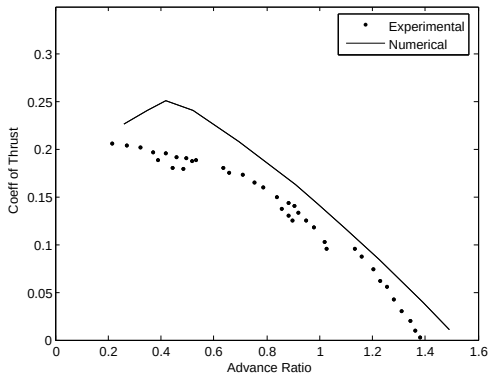

Figure 3: Experimental and numerical results for thrust coefficient vs. advance ratio.

Figure 4a and Fig. 4b display the numerical results vs. the time averaged experimental data taken by Lepicovsky[10]. Only basic parameters of the experimental propeller were included in the publication, so two assumptions were made: 1) the chord has an elliptical distribution, 2) The airfoil has lift and drag characteristics of a NACA 0012. From the deficit in the predicted velocity profiles in Fig. 4a, it is apparent that the propeller had an undisclosed pitch offset. By adding a pitch offset of 10 degrees, Fig. 4b was produced. The absence of a model to predict the slipstream interaction with the freestream is apparent in the numerical results. However, the basic numerical velocity profiles are similar to the experimental results.

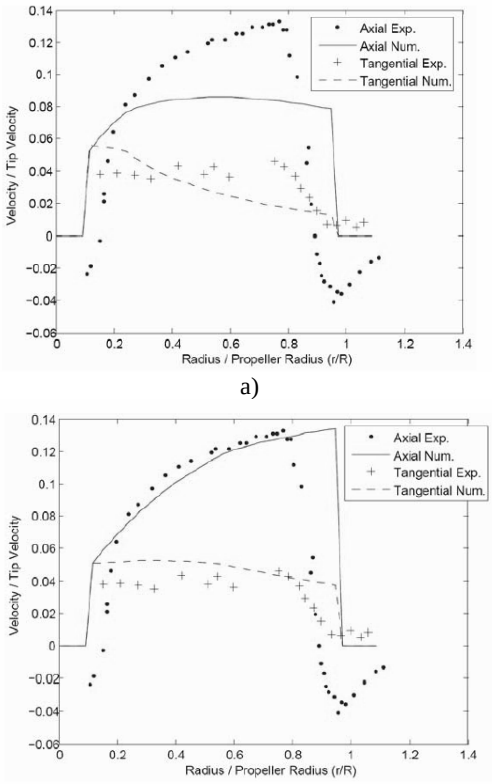

Figure 4: Normalized time-averaged velocities behind propeller vs. normalized propeller radius.

5.3 Results of Combined Models

A scenario was created involving the wing and propeller geometry used by Stuper[8] and seen in Fig. 1. The propeller had a diameter of 15cm and a pitch of 6cm. The propeller was placed in the model 12.5cm in front of the wing quarter chord and spun at an advance ratio of .15 in the 30m/s freestream. Figure 5 shows the resulting prediction for the C_l distribution across the wing.

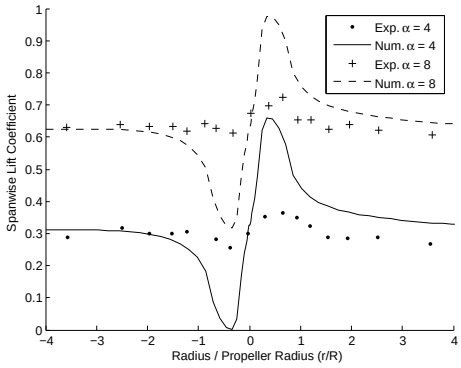

Figure 5: Numerical and experimental results for the C_l distribution along the span of a wing in a propeller slipstream.

Note that the numerical results are qualitatively correct, but quantitatively optimistic. This discrepancy can partially be attributed to the lack of information about the specific prop used; only the standard pitch and diameter were given. It is believed that a more accurate representation of the actual propeller in the model would result in better agreement with the experimental data. Additionally, the numerical lifting-line approach implemented in the aerodynamic model could be optimistically predicting the lift across the wing. Future research will include extensive analysis of this scenario as well as comparing the numerical model predictions to experimental results from Robinson[11] and Brenckmann[12].

6 Conclusion

The aerodynamic model is accurate for lifting surfaces below stall. The accuracy of the propeller model is dependent upon the extent to which the propeller is correctly characterized within the model. Further work will include a study of how this method works for predicting the aerodynamic effects of stall.

The preliminary results presented above indicate that this method shows promise for initial aerodynamic design calculations of wings with significant slipstream effects. Further comparisons will be made to full RANS solutions for both the rotational and nonrotational slipstream scenarios. The speed of this solution along with its accuracy allow it to be linked to a real-time flight simulator. The simulator will provide a test base to assess an autopilot suitable for VTOL aircraft before physical tests are conducted.

References

[1] Lotstedt, P., "Propeller Slip-Stream Model in Subsonic Linearized Potential Flow," *Journal of Aircraft*, Vol. 29, 1992, pp. 1098–1105.

[2] Metcalfe, M., "On the Modelling of a Fully-Relaxed Propeller Slipstream," *AIAA/SAE/ASME/ASEE 21st Joint Propulsion Conference*, 1985.

[3] E.S. Levinsky, H.U. Thommen, P. Y. C. H., "Lifting-Surface Theory for V/STOL Aircraft in Transition and Cruise. I," *Journal of Aircraft*, Vol. 6, 1969, pp. 488–495.

[4] E.S. Levinsky, H.U. Thommen, P. Y. C. H., "Lifting-Surface Theory for V/STOL Aircraft in Transition and Cruise. II," *Journal of Aircraft*, Vol. 7, 1970, pp. 58–65.

[5] Phillips, W. and Snyder, D., "Modern Adaptation of Prandtl's Classic Lifting-Line Theory," *Journal of Aircraft*, Vol. 37, 2000, pp. 662–670.

[6] Prandtl, L. and Betz, A., *Vier Abhandlungen zur Hydrodynamik und Aerodynamik*, Gottingen, 1927.

[7] Stone, R. H., "Aerodynamic Modelling of a Wing-in-Slipstream Tail-Sitter UAV," *AIAA 2002 Biennial International Powered Lift Conference and Exhibit*, 2002.

[8] Stuper, J., "Effect of Propeller Slipstream on Wing and Tail," *NACA TM 874*, 1938.

[9] M.A. Kotb, J. S., "Measurement of Three-Dimensional Turbulent Flow Behind a Propeller in a Shear Flow," *AIAA Journal*, Vol. 24, 1986, pp. 570–577.

[10] J. Lepicovsky, W. B., "Aerodynamic Measurements About a Rotating Propeller with a Laser Velocimeter," *Journal of Aircraft*, Vol. 21, 1984, pp. 264–271.

[11] Robinson, R. G. and William H. Herrnstein, J., "Wing-Nacelle-Propeller Interference for Wings of Various Spans Force and Pressure-Distributuion Tests," *NACA Report No. 569*, 1936.

[12] Brenckmann, M. E., "Experimental Investigation of the Aerodynamics of a Wing in a Slipstream," *Journal of the Aeronautical Sciences*, 1958.